Inorganic Chemistry

pubs.acs.org/IC
Article

CE-ICP-MS Investigation of the Carbonate Complexation of Am(III), Th(IV), Np(V), and U(VI) and the Influence of Alkali Cations

Janik Lohmann, Stefanie Isabella Demel, Justus Carl Sander, and Tobias Reich*

Cite This: *Inorg. Chem.* 2025, 64, 20915−20926
Read Online

ABSTRACT: Capillary electrophoresis inductively coupled plasma mass spectrometry (CE-ICP-MS) was used to investigate the carbonate complexation of Am(III), Th(IV), Np(V), and U(VI) at environmentally relevant concentrations. Experiments were conducted at an ionic strength of 0.33 M in different alkali chloride solutions (Li^+, Na^+, and K^+). Formation constants for the three successive actinide carbonate complexes were determined for Am(III), Np(V), and U(VI). For Th(IV), the CE-ICP-MS measurements posed some challenges. The complexation of U(VI) with carbonate was determined to be stronger than previously assumed. A strong influence of alkali cations on the electrophoretic mobility μ of highly negatively charged actinide carbonate complexes was observed and attributed to the association of cations to those complexes. The electrophoretic mobility of negatively charged An-CO_3 complexes was found to follow the trend $|\mu_{Li}| \leq |\mu_{Na}| < |\mu_K|$. Furthermore, the reaction of $UO_2(CO_3)_3^{4-}$ with different alkali cations ($Me^+ = Li^+ - Cs^+$) was studied. Complex formation constants for $MeUO_2(CO_3)_3^{3-}$ and $Me_2UO_2(CO_3)_3^{2-}$ for all investigated cations were determined.

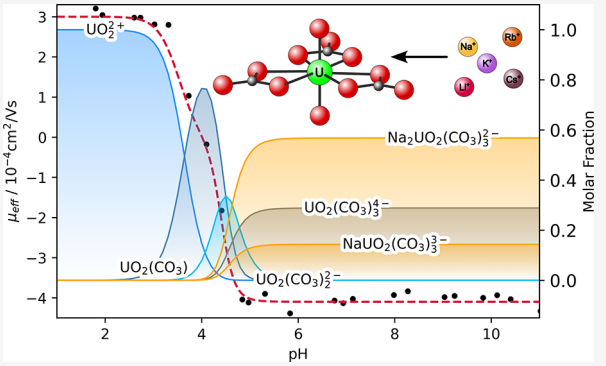

1. INTRODUCTION

For the safety analysis of a high-level nuclear waste repository, it is necessary to investigate the behavior of the long-lived actinides under environmentally relevant conditions. Processes like actinide diffusion and sorption are strongly dependent on the actinide species present.[1] Therefore, it is important to have a thorough understanding of the complexation of actinides, including thermodynamic constants and molecular structures. The Nuclear Energy Agency (NEA) has extensively compiled and reviewed thermodynamic data with their Thermochemical Database (TDB) Project.[2−5] A wide range of experimental methods are needed to produce satisfying thermodynamic data. Experiments at trace-level concentrations, which better reflect the environmentally relevant conditions, are of particular interest.

Due to its ubiquitous nature, carbonate occurs in all surface waters. But also in pore waters underground, significant carbonate concentrations can be present. Opalinus clay pore water for example contains 5×10^{-4} M carbonate.[6] Carbonate is, together with hydroxide, one of the most environmentally relevant ligands regarding actinides and plays a significant role in their mobilization.

Many of the corresponding complex formation constants for the actinides up to Cm are described in literature. The complexation of Am(III) with carbonate was previously studied mainly by solubility experiments[7] or optical methods.[8] In some TLRFS experiments,[9,10] Cm(III) was used as an analog for Am(III). Most studies agree on the formation of three successive An(III) carbonate complexes. For Cm(III), a fourth complex $Cm(CO_3)_4^{5-}$ has been discussed.[10] This complex has not been observed for Am(III) yet.[5] Under a high CO_2 partial pressure >1 bar, the formation of a Cm(III) bicarbonate complex $CmHCO_3^{2+}$ has been observed by Fanghänel et al.[9] While the use of Cm(III) enables experiments at trace concentrations, experiments using Am(III) were done at the solubility limit of Am(III).[5]

Studies investigating the complexation of Th(IV) with carbonates were summarized in the NEA review by Rand et al.[4] Th(IV) has a strong affinity for carbonate as well as hydroxide anions. With its high coordination number, about 20 different binary and ternary complexes are possible.[11] Due to the complexity of the system, there are some inconsistencies in literature concerning the dominating complexes. Altmaier et al.[12] describe the ternary $Th(OH)(CO_3)_4^{5-}$ and $Th(OH)_2(CO_3)_2^{2-}$ complexes as the most important ones, while Östhols et al.[13] describe the $Th(CO_3)_5^{6-}$ complex as dominating at higher pH values. In both studies, the solubility

Received: June 2, 2025
Revised: September 17, 2025
Accepted: September 26, 2025
Published: October 16, 2025

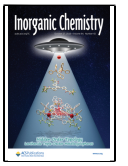

of Th(IV) hydrous oxide was investigated in carbonate solution resulting in Th(IV) concentrations up to 1×10^{-3} M.

The Np(V) carbonate system has been reported extensively in literature.[2] Topin et al.[14] and Aupiais et al.[15] successfully studied the system using a coupling between capillary electrophoresis and inductively coupled plasma mass spectrometry (CE-ICP-MS) at environmentally relevant concentrations (1×10^{-7} M). For Np(V) three successive carbonate complexes are known with $NpO_2(CO_3)_3^{5-}$ being the limiting complex. The formation of ternary Np(V)−CO_3−OH complexes has been discussed in the review done by Lemire et al.,[2] and a value for the formation of the $NpO_2(CO_3)_2OH^{4-}$ complex was selected.

The complexation of U(VI) with carbonate was studied mostly in solubility experiments[3,16−18] with concentrations above 1×10^{-5} M. Three successive U(VI) carbonate complexes were identified along with the polynuclear complex $(UO_2)_3(CO_3)_6^{6-}$. The polynuclear complex becomes irrelevant at lower U(VI) concentrations.

Except for Cm(III) and Np(V) most complexation studies were carried out at significantly higher actinide concentrations than expected in the case of a release of actinides from a waste repository into the environment. CE-ICP-MS is an invaluable tool to investigate the complexation behavior of actinides at trace concentrations.[14,15,19,20] In this work, the complexation behavior of ^{241}Am(III), ^{232}Th(IV), ^{237}Np(V), and ^{238}U(VI) at trace-level with carbonate was investigated by CE-ICP-MS with the aim of determining complex formation constants. The separation capability of the CE, based on charge-to-radius ratio, combined with the mass selectivity of the ICP-MS enabled simultaneous investigations of all four actinides.

In previous CE-ICP-MS studies,[14,15,20] an influence of alkali cation on the electrophoretic mobility of negatively charged carbonate complexes was observed. To further study this effect, in this work the influence of alkali cations Li^+, Na^+, K^+, Rb^+, and Cs^+ on the carbonate complexation was investigated. The charge sensitivity of CE-ICP-MS is ideal for the investigation of potential association reactions.

2. EXPERIMENTAL SECTION

2.1. Determination of Complexation Constants by Capillary Electrophoresis. The determination of complex formation constants by CE is described in detail by Willberger et al.[19] From the CE measurements, migration times of the actinides and the neutral marker for the electroosmotic flow (EOF) were determined. The effective electrophoretic mobility μ_{eff} can be calculated by eq 1 with the migration time of the actinide t_{An}, the migration time of a neutral marker t_{EOF}, indicating the EOF, the effective length l of the capillary and the applied voltage U.

$$\mu_{eff} = \frac{l^2}{U}\left(\frac{1}{t_{An}} - \frac{1}{t_{EOF}}\right) \quad (1)$$

For the carbonate complexation, the exchange between the species present in solution occurs fast in the time frame of the electrophoretic separation, so only one peak with the average mobility of all species present is measured. The measured effective mobility μ_{eff} is therefore made up of the proportions α_i of these species and their corresponding mobilities μ_i (eq 2)

$$\mu_{eff} = \sum_{i=0}^{N} \alpha_i \mu_i \quad (2)$$

The equilibria of actinides Am^{3+} and AnO_2^z (NpO_2^+ and UO_2^{2+}) with carbonate shown in eqs 3 through 6 are assumed. For Am(III), Np(V), and U(VI), the limiting binary carbonate complex is assumed to be the 1:3 complex.

$$Am^{3+} + iCO_3^{2-} \rightleftharpoons Am(CO_3)_i^{3-2i} \quad (3)$$

$$AnO_2^z + iCO_3^{2-} \rightleftharpoons AnO_2(CO_3)_i^{z-2i} \quad (4)$$

In addition, the $AmHCO_3^{2+}$ species, based on the analogy with $CmHCO_3^{2+}$ observed by Fanghänel et al.,[9] (eq 5) and the $NpO_2(CO_3)_2OH^{4-}$ complex (eq 6) are expected to form under the experimental conditions.

$$Am^{3+} + CO_3^{2-} + H^+ \rightleftharpoons AmHCO_3^{2+} \quad (5)$$

$$NpO_2^+ + 2CO_3^{2-} + H_2O \rightleftharpoons NpO_2(CO_3)_2OH^{4-} + H^+ \quad (6)$$

The cumulative complex formation constants β corresponding to eqs 3 through 6 are defined in eqs 7 through 10. The square brackets indicate molar concentration of the reactants.

$$\beta_i = \frac{[Am(CO_3)_i^{3-2i}]}{[Am^{3+}][CO_3^{2-}]^i} \quad (7)$$

$$\beta_{1,H} = \frac{[Am(HCO_3)^{2+}]}{[Am^{3+}][CO_3^{2-}][H^+]} \quad (8)$$

$$\beta_i = \frac{[AnO_2(CO_3)_i^{z-2i}]}{[AnO_2^z][CO_3^{2-}]^i} \quad (9)$$

$$\beta_{2,OH} = \frac{[NpO_2(CO_3)_2OH^{4-}][H^+]}{[NpO_2^+][CO_3^{2-}]^2} \quad (10)$$

Using eq 9 for example, the proportions α_i with i = 1, 2, 3 of the carbonate species present in solution for U(VI) can be expressed by eq 11.

$$\alpha_i = \frac{\beta_i[CO_3^{2-}]^i}{1 + \sum_{x=1}^{3}\beta_x[CO_3^{2-}]^x} \quad (11)$$

Combining eqs 2 and 11, eq 12 is obtained, with which the complex formation constants can be determined from the measured electrophoretic mobility μ_{eff} in relation to the free carbonate concentration $[CO_3^{2-}]$. For Am(III) and Np(V) the corresponding equations are shown in the Supporting Information (eqs S1 and S2, Supporting Information)

$$\mu_{eff} = \frac{\mu_0 + \sum_{i=1}^{3}\mu_i\beta_i[CO_3^{2-}]^i}{1 + \sum_{i=1}^{3}\beta_i[CO_3^{2-}]^i} \quad (12)$$

The electrophoretic mobility of the actinides in absence of carbonate μ_0 is made up of the mobilities of the free actinide as well as the corresponding chloro-complexes. Because chloride concentrations did not change throughout the experiments, the ratio between the free actinide and the actinide chloro complex stays the same and μ_0 can substitute the mobility of the free actinide. Therefore, chloro-complexes are not considered further.

The concentration of free carbonate $[CO_3^{2-}]$ as a function of its initial concentration c_0 and pH can be calculated using eq 13.

$$[CO_3^{2-}] = \frac{c_0}{1 + 10^{(pK_{a2} - pH)} + 10^{(pK_{a1} + pK_{a2} - 2pH)}} \quad (13)$$

The pK_a[5] values of H_2CO_3 were adjusted to an ionic strength of 0.33 M (converted to molality) using the specific ion interaction theory (SIT) and the ion interaction coefficients of the corresponding alkali cation[21] (summarized in SI Table S6). The pK_a values are shown in Table 1. For Li^+ no ion interaction coefficients were found, so the pK_a values were adjusted using data for Na^+.

2.2. CE-ICP-MS. All CE measurements were performed using an Agilent 7100 CE system (Agilent Technologies, Waldbronn, Germany) hyphenated to an Agilent 7900 ICP-MS (Agilent

https://doi.org/10.1021/acs.inorgchem.5c02509
Inorg. Chem. 2025, 64, 20915−20926

Table 1. pK_a Values of Carbonic Acid Adjusted to I = 0.335 m for Li^+, I = 0.333 m for Na^+, and I = 0.335 m for K^+

cation	pK_{a1}^{I}	pK_{a2}^{I}
Li^+, Na^+	6.08	9.71
K^+	6.06	9.77

Technologies, Wiesental, Germany). This coupling was realized via a MiraMist CE nebulizer (Burgener Research, Mississauga, Canada) and a Scott-type spray chamber (AHS Analysentechnik, Tübingen, Germany). To aid the aerosol formation, a makeup electrolyte containing 1.25% HNO_3, 10% ethanol and 5 ppb ^{7}Li, ^{24} Mg, ^{59}Co, ^{89}Y, ^{140}Ce, and ^{205}Tl acting as internal standards was added via the peristaltic pump of the ICP-MS with a flow rate of 15 μL/min. 2-Bromopropane was added to the samples to mark the electroosmotic flow by detecting ^{79}Br by ICP-MS.

For the CE experiments, a fused silica capillary with 50 μm inner diameter and 50 cm length was used (Polymicro Technologies, Phoenix, Arizona, USA). At the start of each experimental series, the capillary was preconditioned using Milli-Q water, 0.1 M HCl, and 0.1 M NaOH. Before each measurement, the capillary was flushed with a background electrolyte (BGE) with the same composition as the sample, but without actinides. Then, 15 nL of the sample were injected hydrodynamically at 100 mbar for 5 s. The capillary was placed back into the BGE and a voltage of 10 kV and a pressure of 60 mbar were applied. The temperature was kept at 25.0 ± 0.1 °C using the internal air cooling of the CE device as well as a custom build enclosure for the hyphenation.

The ICP-MS was used in time-resolved analysis mode for detection with a dwell time of 100 ms and a plasma at 1550 W. The carrier gas flow rate was set to 1 L/min and no makeup gas was used. The detected masses were ^{79}Br, ^{89}Y, ^{127}I, ^{232}Th, ^{237}Np, ^{238}U, and ^{241}Am. In most cases, the peak search of the MassHunter 5.1 software (Agilent Technologies, Santa Clara, California, USA) was used to extract the migration times. For ambiguous peaks, the migration time was selected manually.

2.3. Reagents. **Caution!** ^{232}Th, ^{237}Np, ^{238}U, and ^{241}Am are radioactive elements and require special precautions as well as radiation protection.

All chemicals used were of analytical grade or better. Milli-Q water was used throughout all experiments (18.2 MΩcm, Synergy Millipore water system, Millipore GmbH, Schwalbach, Germany). To prevent clogging, all solutions used were filtered through syringe filters (0.2 μm, Nalgene, Rochester, New York, USA). A list of all suppliers for the chemicals used can be found in SI (Table S5).

An ^{241}Am(III) stock solution was prepared by evaporating an in-house ^{241}Am solution to dryness and redissolving in 0.1 M $HClO_4$. For the ^{237}Np(V) stock solution, an in-house ^{237}Np solution was evaporated until near dryness and redissolved in 1 M $HClO_4$. This process was repeated three times to yield a Np(VI) solution. In the last step, the ^{237}Np was dissolved in 0.1 M $HClO_4$ and $NaNO_2$ was added to reduce the Np(VI) to Np(V). The oxidation state was confirmed by UV−vis spectroscopy (Tidas 100, J&M Analytik AG, Essingen, Germany). The concentrations of the ^{241}Am and ^{237}Np solutions were determined by γ-ray spectroscopy (^{241}Am at 59.5 keV, ^{237}Np at 86.5 keV) using a high-purity germanium detector (GMX-13280-S, ORTEC, Oak Ridge, Tennessee, USA) and the Canberra InSpector 2000DSP Portable Workstation (Model IN2K, Canberra Industries Inc., Meriden, Connecticut, USA). For the ^{232}Th(IV) and ^{238}U(VI) stock solutions, ICP-MS standards (^{232}Th: Accu Trace, Accu Standard, New Haven, Connecticut, USA, ^{238}U: SPEX Certiprep, Metuchen, Massachusetts, USA) of known concentrations were evaporated and redissolved in 0.1 M $HClO_4$. All stock solutions were combined to produce an actinide cocktail with $[^{241}Am] = 3 \times 10^{-5}$ M, $[^{232}Th] = 1 \times 10^{-3}$ M, $[^{237}Np] = 2 \times 10^{-4}$ M, and $[^{238}U] = 2 \times 10^{-4}$ M in 0.1 M $HClO_4$. If not stated otherwise, this actinide cocktail was used throughout all experiments.

2.4. Sample Preparations. For each BGE, the pH value of a 0.1 M Me_2CO_3 solution (Me = Li, Na, K) was varied between pH 2 and pH 11 using HCl. The ionic strength was raised to I = 0.33 M using the corresponding alkali chloride salt. As buffers, 0.05 M MES (2-(*N*-morpholino)ethanesulfonic acid) was added between pH 4 and pH 7, 0.05 M HEPES (4-(2-hydroxyethyl)-1-piperazineethanesulfonic acid) between pH 7 and pH 8, and 0.05 M CHES (*N*-cyclohexyl-2-aminoethanesulfonic acid) between pH 8 and pH 10. No buffer was added below pH 4 and above pH 10. The pH values were measured with an inoLab pH 720 meter (WTW a Xylem brand, Weilheim, Germany) and a BlueLine 16 pH microelectrode (SI Analytics a Xylem brand, Mainz, Germany) filled with 3 M NaCl solution. The device was calibrated with reference buffer solutions at pH 4.01, pH 6.87, and pH 9.18. The detailed composition of each sample can be found in SI (Tables S7, S9, S11, S13). To flush the capillary prior to the CE measurements, 200 μL of each BGE were added to glass vials and capped off using polyethylene snap caps.

The actinide cocktail was diluted using an aliquot of the BGEs to produce the following concentrations: $[^{241}Am] = 3 \times 10^{-8}$ M, $[^{232}Th] = 1 \times 10^{-6}$ M, $[^{237}Np] = 2 \times 10^{-7}$ M, and $[^{238}U] = 2 \times 10^{-7}$ M.

The pH values were remeasured upon actinide addition and readjusted, if necessary. In most samples, no significant change in pH was observed. Directly before each CE-measurement, the pH value was checked again. A portion of 200 μL of the actinide containing sample was transferred to glass vials along with 1 μL of 2-bromopropane as a marker for the EOF.

For the determination of the complex formation constants for the ternary alkali-actinide-carbonate complexes, only U(VI) was chosen for its wide range in pH and carbonate concentration where the $UO_2(CO_3)_3^{4-}$ complex predominates. For this measurement series, BGEs with ionic strengths between I = 0.05 M and I = 0.30 M were prepared by dissolving varying amounts of MeCl (Me = Li, Na, K, Rb, Cs) in 0.005 M Me_2CO_3 solution of the corresponding cation. No buffer was used, and pH values varied between pH 10.3 and pH 10.9. Samples for the CE-ICP-MS measurements were prepared as described above. In addition to the U(VI) stock solution ($[^{238}U] = 2 \times 10^{-7}$ M), an aliquot of 1×10^{-5} M HI was added to monitor the influence of ionic strength on the mobility of I^-.

2.5. Influence of Buffers. To stabilize the pH values between pH 4 and pH 10, the "Good's buffers"[22] MES, HEPES, and CHES were used in this work. Although it is assumed that Good's buffers show only weak affinity toward metal ions,[23,24] data for actinide complexation is sparse at best. It should not be neglected that the buffers could complex actinides via their sulfonate group when discussing complex formation constants. Mandal et al.[25] reported an interaction of several buffers with Eu(III) and even proposed complex formation constants for Eu(MES), $Eu(MES)_2$, and Eu(HEPES) complexes. To check the extend of influence of MES and HEPES on the measurement, complex formation constants proposed by Mandal et al.[25] for Eu(III) as chemical analog for Am(III) were added to the speciation calculation under the experimental conditions present in this work (Figure S1, Supporting Information). In the presence of MES, the $Am(MES)^{2+}$ and $Am(MES)_2^+$ complexes form below 16% and thus hardly influence the trend in mobility (Figure S2, Supporting Information). The $Am(HEPES)^{2+}$ complex is not to be expected in the presence of carbonate. Therefore, the overall influence on the trend in electrophoretic mobility can be neglected. Th(IV) is expected to show the highest affinity for the buffer. In absence of other ligands, an influence of CHES on the mobility of Th(IV) at pH 10 was observed (not shown here). The mobilities measured in the presence of carbonate on the other hand were highly negative for the pH regions where the buffers were applied. Thus, Th(IV)-buffer complexation in the presence of carbonate seems unlikely.

The influence of buffers on Np(V) in the presence of carbonate has been sufficiently discussed by Topin et al.[14] In the pH range where a U(VI)-MES complex would be expected, the carbonate complexation of U(VI) is already well advanced. No influence was observed for HEPES and CHES. It can be summarized that the influence of the buffers used can be neglected for the determination of actinide carbonate complex formation constants.

2.6. Data Treatment. For the determination of complex formation constants, the measured electrophoretic mobilities μ_{eff}

https://doi.org/10.1021/acs.inorgchem.5c02509
Inorg. Chem. 2025, 64, 20915−20926

were plotted against the pH value. By fitting eqs 12, S1, and S2 to the experimental data, complex formation constants log β were obtained, respectively. The fit was performed by a custom Python script using the lm-fit[26] library based on the Levenberg–Marquardt method for nonlinear least-squares minimization. The corresponding correlation matrices are summarized in the SI. To simplify the fitting procedure, the mobilities μ_i of each species were fixed and varied separately. For the determination of μ_i, the following conditions were applied:

(1) Positively charged complexes have positive mobilities and negatively charged complexes have negative mobilities.
(2) For neutral complexes, the electrophoretic mobility is fixed at zero.
(3) Electrophoretic mobilities decrease with the number of carbonate ligands associated with the actinide.
(4) If the trend in electrophoretic mobility shows a plateau at high $[CO_3^{2-}]$ corresponding to the limiting complex, the value of the plateau is assumed to represent the mobility of the corresponding predominant complex and is fixed.

If not stated otherwise, all obtained complex formation constants were extrapolated to zero ionic strength using SIT.[21] For this purpose, the ionic strength of I = 0.33 M was converted to molality units I = 0.333 mol/kg$_w$ using the density of the NaCl solution calculated as described in Novotny and Sohnel.[27] The other electrolytes were treated analogously. The ion interaction coefficients used in this work are summarized in SI (Table S6).

3. RESULTS AND DISCUSSION

3.1. Carbonate Complexation. All electropherograms measured in NaCl can be found in SI (Figures S11 and S12). With eq 1, the effective electrophoretic mobilities μ_{eff} were calculated for each actinide (Table S8, Supporting Information). The electrophoretic mobilities μ_{eff} of Am(III), Np(V), and U(VI) were plotted against the pH as shown in Figure 1.

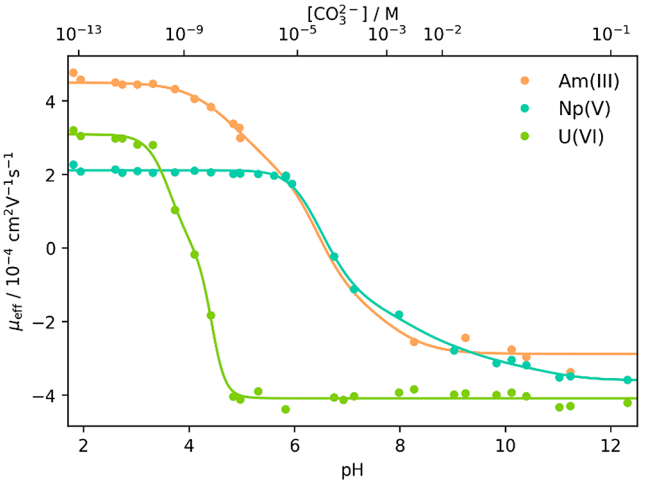

Figure 1. Measured effective electrophoretic mobilities μ_{eff} of ^{241}Am(III), ^{237}Np(V), and ^{238}U(VI) plotted against pH as well as the free carbonate concentration $[CO_3^{2-}]$ at I = 0.333 m in NaCl with applied fit (solid lines) according to eqs 12, S1, and S2. R^2_{Am} = 0.997, R^2_{Np} = 0.998, and R^2_U = 0.998.

Clear progressions of μ_{eff} as a function of pH and carbonate concentration were observed for all actinides. The individual mobilities assigned to the actinide carbonate complexes are summarized in Table 2. Because of actinide chloride complexes, the electrophoretic mobility μ_0 in absence of carbonate is made up of the mobility of the free actinide and the mobility of the chloride complex. The average charge z of $(An^{z+} + AnCl^{z-1})$ given in Table 2 was calculated based on the proportions determined using PhreeQC[28] and ThermoChimie v12a.[29]

Table 2. Assumed Electrophoretic Mobilities μ of the Individual Species Investigated[a]

species	z	$\mu/10^{-4}$ cm^2/(Vs)	$Q/10^4$ Vs/cm^2
$Am^{3+} + AmCl^{2+}$	2.93	4.50	0.65
$Am(HCO_3)^{2+}$	2	3.00	0.67
$Am(CO_3)^+$	1	1.53	0.65
$Am(CO_3)_2^-$	−1	−1.53	0.65
$Am(CO_3)_3^{3-}$	−3	−2.90	1.03
NpO_2^+	1	2.11	0.47
$NpO_2(CO_3)^-$	−1	−1.64	0.61
$NpO_2(CO_3)_2^{3-}$	−3	−2.72	1.10
$NpO_2(CO_3)_2OH^{4-}$	−4	−3.59	1.11
$NpO_2(CO_3)_3^{5-}$	−5	−3.90	1.28
$UO_2^{2+} + UO_2Cl^+$	1.90	3.09	0.61
$UO_2(CO_3)_{(aq)}$	0	0	-
$UO_2(CO_3)_2^{2-}$	−2	−3.28	0.61
$UO_2(CO_3)_3^{4-}$	−4	−4.09	0.98

[a]The ionic charge of the species is z. For Q see eq 16 below.

3.1.1. Americium(III). The trend in electrophoretic mobility (Figure 1) for Am(III) starts and ends in a plateau. The corresponding values were selected as μ_0 at low carbonate concentration and μ_3 of the limiting 1:3 complex at high carbonate concentration. Values for the assumed mobilities of all actinide complexes investigated are summarized in Table 2. The mobility of $Am(CO_3)_3^{3-}$ agrees with the mobility of Eu(III) measured by Philippini et al.[20] using CE-ICP-MS at $[Na_2CO_3]$ = 0.15 M. Between pH 5 and 8 electropherograms of Am did not show reliable peaks. This range of pH coincides with the pH range Chung et al.[30] observed the formation of Cm(III)-SiO surface complexes in 0.5 g/L amorphous silica solution. Therefore, a strong interaction or sorption of Am(III) on the fused silica capillary is likely responsible for the loss of signal. In this pH range the $Am(CO_3)_2^-$ complex is expected to dominate. The lack of data points made it impossible to determine the complex formation constant of the 1:2 complex. For the fit of the data, the corresponding constant was expressed as $\log \beta_2^{0.333m} = \log \beta_1^{0.333m} + \log K_2^{0.333m}$ with $\log K_2^{0.333m}$ = 4.29, the value selected by Guillaumont et al.,[3] extrapolated to I = 0.333 m, and fixed. At pH > 8 clear peaks for Am were observed, indicating that the formation of the 1:3 Am-CO_3 complex reduces the sorption on the fused silica. The calculated complex formation constants log β_i are summarized in Table 3.

The calculated log β^0 value for the $Am(HCO_3)^{2+}$ complex agrees with the value for the $Cm(HCO_3)^{2+}$ complex selected in the NEA review done by Guillaumont et al.[3] based on the experiments by Fanghänel et al.[9] The obtained log β^0 values for the $Am(CO_3)^+$ and $Am(CO_3)_3^{3-}$ complexes also agree with the ones selected by Guillaumont et al.[3] within the margin of error. To further compare the obtained values with the literature, the specific interaction equation[21] was applied to the data compiled by Guillaumont et al.[3] including the values determined in this work in Figure S3 in the SI. The inclusion of the values determined in this work does not change the values selected by Guillaumont et al.[3] significantly.

3.1.2. Neptunium(V). The measured electrophoretic mobilities for Np(V) are in good agreement with the CE-ICP-MS study by Topin et al.[14] under similar conditions (I = 0.37 M). The mobilities of Np(V) are constant up to pH 5.5 (Figure 1).

https://doi.org/10.1021/acs.inorgchem.5c02509
Inorg. Chem. 2025, 64, 20915−20926

Table 3. Complex Formation Constants $\log \beta_i$ for Am(III)-Carbonate Complexes at I = 0.333 m and Zero Ionic Strength as well as Values Selected in the NEA Review Done by Guillaumont et al.[3]

reaction	$\log \beta^{0.333m}$	$\log \beta^0_{SIT}$	$\log \beta^0_{NEA}$[3]
$Am^{3+} + CO_3^{2-} + H^+ \rightleftharpoons Am(HCO_3)^{2+}$	12.20 ± 0.20	13.74 ± 0.20	13.43 ± 0.30[a]
$Am^{3+} + CO_3^{2-} \rightleftharpoons Am(CO_3)^+$	6.69 ± 0.23	8.53 ± 0.23	8.00 ± 0.40
$Am^{3+} + 2CO_3^{2-} \rightleftharpoons Am(CO_3)_2^-$	10.98[b]	13.43	12.90 ± 0.60
$Am^{3+} + 3CO_3^{2-} \rightleftharpoons Am(CO_3)_3^{3-}$	13.84 ± 0.36	15.66 ± 0.36	15.00 ± 0.50[c]

[a]Calculated from selected data in Guillaumont et al.[3] to match eq 5. [b]Fixed at $\log \beta_2^{0.333m} = \log \beta_1^{0.333m} + \log K_2^{0.333m}$ with $\log K_2^{0.333m} = 4.29$ extrapolated to I = 0.333 m from the value selected by Guillaumont et al.[3] and fixed. [c]The value was retained by the latest NEA review done by Grenthe et al.[5] but the uncertainty was decreased.

Table 4. Complex Formation Constants $\log \beta_i$ for Np(V)-Carbonate Complexes at I = 0.333 m and Zero Ionic Strength as well as Values Selected in the NEA Reviews Done by Lemire et al.[2] and Guillaumont et al.[3] and Reported by Topin et al.[14] and Aupiais et al.[15]

reaction	$\log \beta^{0.333m}$	$\log \beta^0_{SIT}$	$\log \beta^0_{NEA}$[2,3]	$\log \beta^0_{Topin}$[14]	$\log \beta^0_{Aupiais}$[15]
$NpO_2^+ \pm CO_3^{2-} \rightleftharpoons NpO_2(CO_3)^-$	4.24 ± 0.04	4.81 ± 0.04	4.96 ± 0.06	4.88 ± 0.12	4.94 ± 0.08
$NpO_2^+ + 2CO_3^{2-} \rightleftharpoons NpO_2(CO_3)_2^{3-}$	6.68 ± 0.14	6.59 ± 0.14	6.53 ± 0.10	6.56 ± 0.10	6.45 ± 0.21
$NpO_2^+ + 3CO_3^{2-} \rightleftharpoons NpO_2(CO_3)_3^{5-}$	7.51 ± 0.23	5.49 ± 0.23	5.50 ± 0.11	5.64 ± 0.15	5.54 ± 0.11
$NpO_2^+ + 2CO_3^{2-} + H_2O \rightleftharpoons NpO_2(CO_3)_2OH^{4-} + H^+$	−3.88 ± 0.42	−5.20 ± 0.42	−5.31 ± 1.17[a]	-	-

[a]Calculated from selected data in Guillaumont et al.[3] to match eq 6.

Table 5. Complex Formation Constants $\log \beta_i$ for U(VI)-Carbonate Complexes at I = 0.333 m and Zero Ionic Strength as well as Values Selected in the NEA Review Done by Guillaumont et al.[3]

reaction	$\log \beta^{0.333m}$	$\log \beta^0_{SIT}$	$\log \beta^0_{NEA}$[3]
$UO_2^{2+} + CO_3^{2-} \rightleftharpoons UO_2(CO_3)_{(aq)}$	9.52 ± 0.08	10.74 ± 0.08	9.94 ± 0.03
$UO_2^{2+} + 2CO_3^{2-} \rightleftharpoons UO_2(CO_3)_2^{2-}$	17.13 ± 0.27	18.37 ± 0.27	16.61 ± 0.09
$UO_2^{2+} + 3CO_3^{2-} \rightleftharpoons UO_2(CO_3)_3^{4-}$	25.30 ± 0.19	25.31 ± 0.19	21.84 ± 0.04

The value of this plateau was assigned to μ_0 of NpO_2^+. At pH > 11 the electrophoretic mobility reaches plateau. The corresponding mobility was assigned to the $NpO_2(CO_3)_2OH^{4-}$ complex. The $NpO_2(CO_3)_3^{5-}$complex only forms to a proportion <30%. This made an assignment of a mobility μ_3 to the 1:3 complex difficult. The value for μ_3 was determined as described by Topin et al.[14] (see Table 2). In the preliminary fits, the free parameter β_3 was constrained within the associated uncertainties of the value proposed by the NEA[2] The calculated complex formation constants log β_i for the Np(V) complexes are summarized in Table 4.

The calculated complex formation constants of the binary Np(V)-carbonate complexes agree with those of the NEA[2] as well as of Topin et al.[14] and Aupiais et al.,[15] showing the reproducibility of CE-ICP-MS when determining complex formation constants. Due to the agreement with data selected by Lemire et al.,[2] applying the NEA procedure to determine the log β^0 was not necessary. The $NpO_2(CO_3)_2OH^{4-}$complex was not determined by Topin et al.[14] and Aupiais et al.[15] The complex formation constant determined in this works agrees closely with the value selected by Lemire et al.[2]

3.1.3. Uranium. The trend in electrophoretic mobility for U(VI) starts and ends in a plateau (Figure 1). The corresponding μ_{eff} values were selected as μ_0 at low carbonate concentration and μ_3 of the limiting 1:3 complex at high carbonate concentration, respectively (Table 2).

The complex formation constants for U(VI) deviate from literature[3] (Table 5). The successive formation constants K_1^0 and K_2^0 deviate about one order of magnitude, while K_3^0 deviates two orders of magnitude. According to the present work, the U(VI) carbonate complexation is stronger than previously assumed. The U(VI) carbonate system has been studied extensively in literature through solubility experiments[16−18] with the lowest U(VI) concentrations around 3 × 10^{-5} M. At these concentrations, polynuclear U(VI) complexes have a great influence on the speciation.[31] At the U(VI) concentration used in this work, polynuclear complexes are unlikely. Solubility experiments are also highly dependent on the characterization of solid phase,[5] whereas with CE-ICP-MS complex formation can be studied directly in the liquid phase.

3.1.4. Thorium. In contrast to the other actinides investigated, thorium only produced clear peaks at pH < 2.6. At pH values above 2.6, peaks in the electropherograms of ^{232}Th started to show a lot of tailing or were interrupted (Figures S11 and S12, Supporting Information). Because of this, electrophoretic mobilities were difficult to determine. Samples were measured directly after Th(IV) addition, remeasuring the samples produced worse signals with clear signs of precipitation and colloid formation[32] (see Figure S4, Supporting Information). The significant amount of tailing indicates a retention of Th(IV) on the fused silica of the capillary via surface complexation. In such cases the front of the signal was assumed to be only governed by electrophoretic mobility. For those reasons, the obtained electrophoretic mobilities are not sufficiently reliable for the determination of complex formation constants.

Nevertheless, a reproducible trend in Th(IV) mobility was observed as shown by the data points in Figure 2. To verify this trend in μ_{eff}, the electrophoretic mobility was modeled using the complex formation constants proposed in the NEA review

https://doi.org/10.1021/acs.inorgchem.5c02509
Inorg. Chem. 2025, 64, 20915−20926

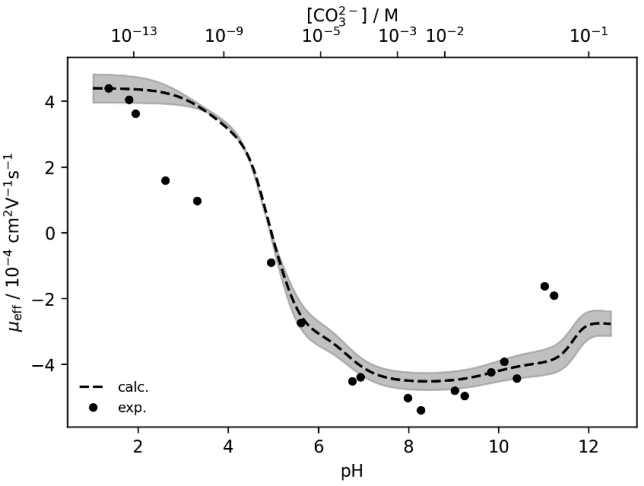

Figure 2. Measured effective electrophoretic mobilities μ_{eff} of ^{232}Th(IV) (dots) plotted against pH value and $[CO_3^{2-}]$ concentration. For comparison, μ_{eff} was estimated based on eq 15 using β_i values selected in the NEA review by Rand et al.[4] (dashed line). The shaded area represents the uncertainty of log β values and a 90% confidence interval for the estimated mobilities.

by Rand et al.[4] extrapolated to I = 0.333 m (see Figure 2 dashed line). Th(IV) has a strong tendency to hydrolyze and to form ternary complexes which can be generalized by eq 14.

$$Th^{4+} + yOH^- + iCO_3^{2-} \rightleftarrows Th(OH)_y(CO_3)_i^{4-y-2i} \quad (14)$$

Equation 12 was extended accordingly to account for the ternary complexes (eq 15).

$$\mu_{eff} = \frac{\mu_0 + \sum_{y,i} \mu_{y,i}\beta_{y,i}[OH^-]^y[CO_3^{2-}]^i}{1 + \sum_{y,i} \beta_{y,i}[OH^-]^y[CO_3^{2-}]^i} \quad (15)$$

The hydroxide concentration was calculated using $[OH^-] = 10^{-(pK_W^{0.333m} - pH)}$ with pK_W = 13.73 at 0.333 m NaCl.

It is not feasible to include all possible binary and ternary Th(IV) complexes to model the experimental data. The most important complexes were identified from speciation calculations using PhreeQC[28] and ThermoChimie v12a[29] (Figure S5, Supporting Information) and are listed in Table S1, Supporting Information. Unlike the other investigated actinides, the Th(IV) mobility does not show a plateau at low carbonate concentrations, so $\mu_0 = 4.39 \times 10^{-4}$ cm^2/(Vs) was estimated based on the measurement at pH 1.34, where no hydrolysis of the Th(IV) is expected. For the Th−OH complexes, the mobilities were estimated based on the μ_0 value and the change in ionic charge. The mobilities of the binary and ternary Th(IV)−CO_3 complexes were assigned based on the mobilities of other actinide species with the same charge (see Table 2). For the $Th(CO_3)_5^{6-}$ complex, there is no equivalently charged complex of the other actinides, so its mobility was estimated to be -5.4×10^{-4} cm^2/(Vs).

As can be seen from Figure 2, a sharp decrease in the measured electrophoretic mobility in the pH range 2−3 was observed in deviation from the calculated values based on the NEA[4] data. In this pH range the hydrolysis of Th(IV) is negligible and a plateau in Th(IV) mobility is expected. The observed decrease in mobility coincides with an increase in sorption of [Th] = 3×10^{-5} M on 4.8 g/L amorphous SiO_2 in 1.0 M $NaClO_4$ between pH 2 and 3 observed by Östhols.[33] Therefore, the decrease in electrophoretic mobility at low pH could be attributed to the surface complexation of Th(IV) on the fused silica of the capillary. The formation of Th−OH−CO_3 complexes lead to a desorption of the Th. Between pH 5 and 10.5, the experimental data could be modeled well using literature data. Starting at pH 10, the mobility should become less negative due to the reduction in charge by formation of $Th(OH)_4(CO_3)^{2-}$ and $Th(OH)_3(CO_3)^-$. This reduction is seen in the experimental data, while the measured electrophoretic mobility around pH 11 deviates from the calculation either due to inaccurately assigned mobilities or a stronger contribution of the neutral $Th(OH)_4$ complex. Nevertheless, it was shown that the change in measured mobility can be explained to some extent with the literature values and the assumption of individual mobilities based on other actinide species.

To produce reliable measurements for the Th-OH-CO_3 system, the experiments have shown that fused silica capillaries are not suitable. Recently, Sun et al.[34] successfully utilized polyetheretherketone (PEEK) capillaries to reduce surface interaction while studying the Ca-U(VI)-CO_3 system.

3.1.5. Electrophoretic Mobilities. Electrophoretic mobility is proportional to the charge-to-size ratio $\left(\frac{z}{r}\right)$ of the ions. To investigate the proportionality between the charge z and the mobility μ of a given species, to potentially see changes in ionic size r, a quotient Q is introduced as follows

$$Q = \frac{z}{\mu} \quad (16)$$

Most species investigated in this work have a Q value between 0.61 and 0.67 $\times 10^4$ Vs/cm^2 (Table 2). Plotting the mobilities μ of the species investigated against the corresponding ionic charge z shows the linear progression more clearly (Figure 3).

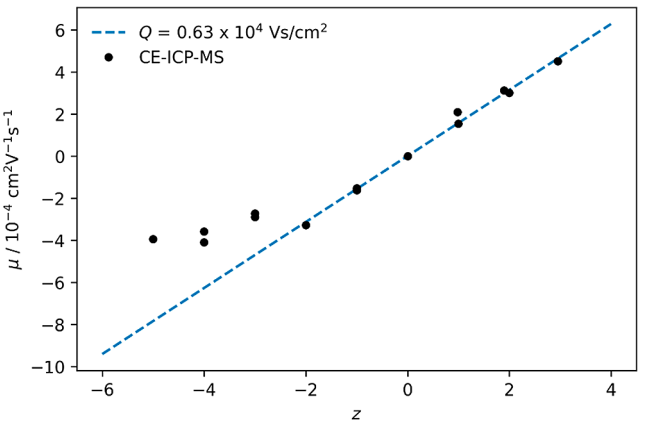

Figure 3. Individual mobilities μ of the species investigated in this work plotted against the corresponding ionic charge z. The blue line indicates a Q value of 0.63 $\times 10^4$ Vs/cm^2.

For complexes with ionic charges between +3 and −2, the mobility follows a linear trend. A linear regression of the determined values in this range produces a Q value of (0.63 ± 0.01) $\times 10^4$ Vs/cm^2. As Q is proportional to the ionic size r, it can be assumed that the association of carbonate ligands does not change the hydrodynamic radius of the complex species significantly as water molecules from the first hydration sphere are displaced.

https://doi.org/10.1021/acs.inorgchem.5c02509
Inorg. Chem. 2025, 64, 20915−20926

For ionic charges below −2, the electrophoretic mobility deviates from the linear trend toward a less negative charge. This deviation increases with the negative charge of the complexes. This effect was also noticed by Aupiais et al.[15] for CE-ICP-MS measurements of Pu(V) in the carbonate system. Aupiais et al.[15] attributed this change in mobility to a change in the binding motive from a bidentate coordination of the first two carbonate ligands to a monodentate coordination for the third ligand resulting in an increase of the coordination sphere. In the present study, the mobility of the $NpO_2(CO_3)_2^{3-}$ complex also shows a deviation from $Q = 0.63 \times 10^4$ Vs/cm^2, although no change in the binding motif was observed for this complex by Aupiais et al.[15] EXAFS studies showed a bidentate binding motive for all carbonate ligands in the limiting carbonate complexes of U(IV),[35] Np(V),[36] U(VI),[37] as well as in DFT studies for Am(III).[38] Without a change in binding motif, it is unlikely that the last carbonate ligand changes the hydrodynamic radius significantly. Another explanation, while also unlikely, could be the formation of ternary An-OH-CO_3 complexes not described in previous literature and in turn a wrong assignment of anionic charge. As most of the formation constants determined in this work agree with previous literature, another effect might cause this deviation. Highly negative complexes are unlikely to be stable in aqueous solution and tend to reduce their negative charge by association with cations present in solution to form ternary alkali-actinide-carbonate complexes as proposed by Topin et al.[14] For U(VI),[39] the association of 3.2 ± 0.7 Na^+ ions to $UO_2(CO_3)_3^{4-}$ at a U−Na distance of 3.82 Å was observed using EXAFS. For U(IV),[35] EXAFS measurements in solution suggest the association of 2 or 3 Na^+ ions to $U(CO_3)_5^{6-}$ at a U−Na distance of 3.62 Å. The formation of Na-$UO_2(CO_3)_3^{4-}$ ion pairs accompanied by a change in binding motif has also been proposed in theoretical calculations.[40] To investigate this association further, the CE-ICP-MS experiments were extended to other alkali cations.

3.2. Influence of Alkali Cations. *3.2.1. Uranium.* Due to the wide range of pH values as well as carbonate concentrations at which the $UO_2(CO_3)_3^{4-}$ complex is predominant, it is particularly suitable for further investigations into the effect of alkali cations. The mobility of ^{238}U(VI) was measured in 5 mM Me_2CO_3 solution at different ionic strengths using LiCl, NaCl, KCl, RbCl, and CsCl. All electropherograms can be found in SI (Figures S15 and S16, Supporting Information). With eq 1 the effective electrophoretic mobilities μ_{eff} were calculated for each electrolyte (Table S13, Supporting Information). The effective electrophoretic mobilities of U(VI) are shown in Figure 4.

The trend in mobility was found to be $|\mu_{Li}| \leq |\mu_{Na}| < |\mu_K| < |\mu_{Rb}| \approx |\mu_{Cs}|$. This trend was also observed by Philippini et al.[20] for lanthanide carbonate complexes in different alkali chloride media (Li−K, Cs). For Li^+, Na^+, and K^+ the effective mobility decreases significantly while for Rb^+ and Cs^+ the mobility only decreases slightly with increasing ionic strength or rather cation concentration. Iodide was added to the measurement to investigate the influence of the ionic strength on the electrophoretic mobility of negatively charged ions in general. It is expected that I^- does not form complexes with alkali ions under the experimental conditions. No apparent influence of the ionic strength or cation concentration on the mobility of I^- was noticed for the range investigated (Figure 4). Because of the higher anion charge of $UO_2(CO_3)_3^{4-}$ compared to I^-, the ionic strength has a more significant influence on the activity of

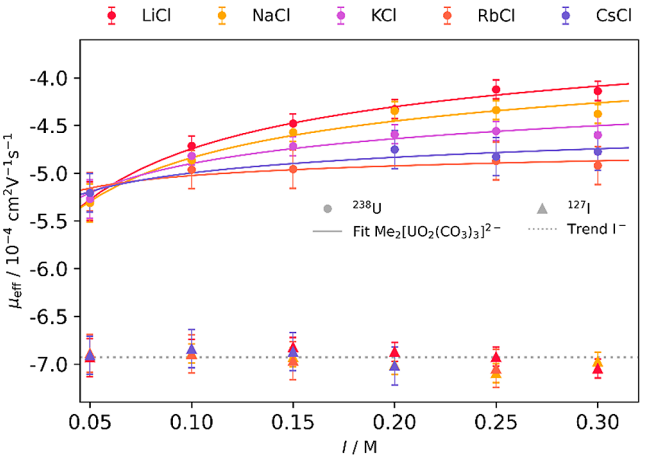

Figure 4. Measured effective electrophoretic mobilities μ_{eff} of ^{127}I and ^{238}U(VI) with $[CO_3^{2-}]$ = 5 mM in LiCl, NaCl, KCl, RbCl, and CsCl at pH between 10.3 and 10.9, plotted against the ionic strength with applied fit according to eq 19. $R^2_{Li} = 0.992$, $R^2_{Na} = 0.964$, $R^2_K = 0.865$, $R^2_{Rb} = 0.868$, and $R^2_{Cs} = 0.932$.

$UO_2(CO_3)_3^{4-}$ and in turn also possibly on the electrophoretic mobility. The formation of stable alkali complexes could superimpose the effect of ionic strength on mobility. For the following calculations, the effect of ionic strength on electrophoretic mobility in the investigated range is neglected. The change in electrophoretic mobility is only attributed to the formation of two ternary Me-U(VI)-CO_3 complexes based on eqs 17 and 18. These equilibria are described by the complex formation constant K_x

$$K_1: \quad Me^+ + UO_2(CO_3)_3^{4-} \rightleftharpoons MeUO_2(CO_3)_3^{3-} \tag{17}$$

$$K_2: \quad Me^+ + MeUO_2(CO_3)_3^{3-} \rightleftharpoons Me_2UO_2(CO_3)_3^{2-} \tag{18}$$

To calculate the complex formation constants K_x of the 1:1:3 and 2:1:3 $Me_xUO_2(CO_3)_3^{x-4}$ complexes based on the mobilities shown in Figure 4, a function analogous to eq 12 was used.

$$\mu_{eff} = \left\{ \mu_{UO_2(CO_3)_3^{4-}} + \mu_{MeUO_2(CO_3)_3^{3-}} \times K_1^I \times [Me^+] + \mu_{Me_2UO_2(CO_3)_3^{2-}} \times K_1^I \times K_2^I \times [Me^+]^2 \right\} / \left\{ 1 + K_1^I \times [Me^+] + K_1^I \times K_2^I \times [Me^+]^2 \right\} \tag{19}$$

This equation is similar to that used by Sun et al.[34] to investigate the complexation of Ca^{2+} with $UO_2(CO_3)_3^{4-}$. In contrast to Ca^{2+} in the experiments of Sun et al.,[34] the alkali cations contribute predominantly to the ionic strength. Because of the varying ionic strength in the experiment, an extrapolation to zero ionic strength after the fit is not feasible. Instead, the complex formation constant at zero ionic strength K^0 is extrapolated to the ionic strength of each data point using SIT[21] (eq 20). This way, the complex formation constants resulting from the fit are already extrapolated to zero ionic strength. The parameters Δz^2 and $\Delta\varepsilon$ are summarized in Table 6.

$$\log K_x^I = \log K_x^0 + \Delta z^2 \times \left(\frac{0.509\sqrt{I_m}}{1 + 1.5\sqrt{I_m}} \right) - \Delta\varepsilon \times I_m \tag{20}$$

https://doi.org/10.1021/acs.inorgchem.5c02509
Inorg. Chem. 2025, 64, 20915−20926

Table 6. Parameters Used for the Extrapolation of log K to a Given Ionic Strength

		1:1:3		2:1:3	
cation	ε (j, Cl^-)	$\Delta\varepsilon$	Δz^2	$\Delta\varepsilon$	Δz^2
Li^+	0.10	−0.10	−8	−0.11	−6
Na^+	0.03	−0.03	−8	−0.04	−6
K^+	0.00	0.00	−8	−0.01	−6
Rb^+	0.00[a]	0.00	−8	−0.01	−6
Cs^+	0.00[a]	0.00	−8	−0.01	−6

[a] $\varepsilon(j, Cl^-)$ of Rb^+ and Cs^+ were estimated assuming $\varepsilon(K^+, Cl^-) = \varepsilon(Rb^+/Cs^+, Cl^-)$.

The ion interaction parameters for the $Me_xUO_2(CO_3)_3^{x-4}$ complexes are not known in literature. For $Me_2UO_2(CO_3)_3^{2-}$, the ion interaction parameter of $\varepsilon(UO_2(CO_3)_2^{2-}, Na^+) = -0.02$ was used. As there is only a small change from $\varepsilon(UO_2(CO_3)_2^{2-}, Na^+) = -0.02$ to $\varepsilon(UO_2(CO_3)_3^{4-}, Na^+) = -0.01$, the latter value was used for the $MeUO_2(CO_3)_3^{3-}$ complex. It has to be noted that it is highly likely that the coefficients differ for the different cations. Since there is no literature, the coefficients of the U(VI) complexes remained constant regardless of the cation for the evaluation. To simplify the evaluation, the molar ionic strength was equated with the molal ionic strength $I_M = I_m$. This introduces a bias of at most 2% at 0.3 M CsCl and is therefore negligible.

Because of the carbonate in solution, the cation concentration deviated from the ionic strength as $[Me^+] = I - 0.005$ M. The calculated complex formation constants K_x^0 are summarized in Table 7. The mobilities for the unassociated and associated complexes were calculated based on their ionic charge with eq 16 and a Q value of 0.63×10^4 Vs/cm^2 (see Table 8).

Since the association of alkaline earth cations Mg^{2+}−Ba^{2+} to $UO_2(CO_3)_3^{4-}$ was already investigated thoroughly in literature,[5] the values selected by the NEA[5] are listed in Table S2. In comparison, the log K^0 values for alkali metals are smaller than the log K^0 values for alkaline earth metals, which is plausible when considering the charge of the cations.[5]

For the $MeUO_2(CO_3)_3^{3-}$ complexes, log K_1^0 increases from Li^+ to Rb^+ and Cs^+. The log K_2^0 values of $Me_2UO_2(CO_3)_3^{2-}$ show an opposing unexpected trend with a decrease from Li^+ to Rb^+ and Cs^+. For the latter two cations log K_1^0 as well as log K_2^0 are similar within the margin of error. This trend is further illustrated in the plot of log K^0 against the reciprocal ionic radius $1/r$[41] (Figure S6, Supporting Information). The observed trends in log K^0 cannot easily be explained by trends in ionic or hydrodynamic radii. To fully understand the system, molecular dynamics calculations similar to the work of Li et al. for Na^+[40] are necessary for all investigated cations.

Overall, it must be noted that complex formation constants in the present work were calculated based on trends in electrophoretic mobilities, excluding further effects of ionic strength on said mobilities. The choice of electrophoretic mobility has an influence on the calculated complex formation constants. Nevertheless, the effect of the alkali cations on the $UO_2(CO_3)_3^{4-}$ complex was clearly demonstrated and represents a starting point for further investigations.

To check for consistency of the new complex formation constants (Table 7), they were fitted to the data of the experiment at varied pH values (Figure 1). In addition, this experiment was repeated analogously in $LiCl/Li_2CO_3$ and KCl/K_2CO_3 solutions. All electropherograms can be found in SI (Figures S13 and S14, Supporting Information). With eq 1 the effective electrophoretic mobilities μ_{eff} were calculated for each actinide (Tables S10, S12, Supporting Information). The measured effective electrophoretic mobilities of U(VI) and the corresponding fits are shown in Figure 5.

The electrophoretic mobility μ_{eff} for U(VI) in Figure 5 exhibits the same trend as observed in Figure 4 with an increase in mobility for the measurement in KCl at high $[CO_3^{2-}]$ compared to the measurements in LiCl and NaCl.

To check the plausibility of the constants K_1 and K_2 (Table 7), the $MeUO_2(CO_3)_3^{3-}$ and $Me_2UO_2(CO_3)_3^{2-}$ complexes were added to eq 12 to obtain eq 21.

$$\mu_{eff} = \left\{ \mu_0 + \sum_i^3 \mu_i \beta_i [CO_3^{2-}]^i + \mu_{1,3} \beta_3 K_1 [CO_3^{2-}]^3 [Me^+] + \mu_{2,3} \beta_3 K_1 K_2 [CO_3^{2-}]^3 [Me^+]^2 \right\} / \left\{ 1 + \sum_i^3 \beta_i [CO_3^{2-}]^i + \beta_3 K_1 [CO_3^{2-}]^3 [Me^+] + \beta_3 K_1 K_2 [CO_3^{2-}]^3 [Me^+]^2 \right\} \quad (21)$$

For the fits shown in Figure 5, all electrophoretic mobilities of the U(VI) species, except for μ_0, were calculated with a Q value of 0.63×10^4 Vs/cm^2 and were fixed during the fitting procedure (Table 8). The value for μ_0 was again derived from the plateau at low $[CO_3^{2-}]$ in NaCl (see Table 2). The complex formation constants log K^0 of the $MeUO_2(CO_3)_3^{3-}$ and $Me_2UO_2(CO_3)_3^{2-}$ complexes in Table 7 were adjusted to I = 0.33 M (converted to molality) using SIT and fixed during the fitting procedure (Table 8). The concentration of the alkali cations was $[Me^+]$ = 0.3 M for the experiment. The electrophoretic mobilities, the adjusted log K^I values, and the complex formation constants log β_i of the U(VI)-CO_3 complexes at I = 0.33 M (converted to molality) are summarized in Table 8.

Within the margin of error, the log β_i values for the 1:1 and 1:2 complexes in Table 8 coincide roughly with each other regardless of the alkali cation as well as with the log β_i values determined in Table 5 without the consideration of the ternary Me-U(VI)-CO_3 complexes. This shows that the alkali cation has next to no influence on the first two U(VI)-CO_3 complexes. For the complex $UO_2(CO_3)_{(aq)}$, this is to be expected. Small differences in log β_i values compared to the values in Table 5 can be attributed to the slightly different mobility of the 1:2 complex.

For the 1:3 complex, the β_3 value determined under consideration of the ternary Me-U(VI)-CO_3 complexes is about one order of magnitude smaller compared to the value

Table 7. Complex Formation Constants log K_x^0 for the Association of Alkali Cations to $UO_2(CO_3)_3^{4-}$ at Zero Ionic Strength

species	log K_{Li}^0	log K_{Na}^0	log K_K^0	log K_{Rb}^0	log K_{Cs}^0
$MeUO_2(CO_3)_3^{3-}$	1.07 ± 0.31	1.47 ± 0.28	2.00 ± 0.14	2.42 ± 0.09	2.25 ± 0.13
$Me_2UO_2(CO_3)_3^{2-}$	2.50 ± 0.31	2.05 ± 0.27	1.44 ± 0.14	0.55 ± 0.21	0.97 ± 0.16

https://doi.org/10.1021/acs.inorgchem.5c02509
Inorg. Chem. 2025, 64, 20915−20926

Table 8. Complex Formation Constants $\log \beta_i$ for U(VI)-Carbonate Complexes and $\log K_i$ for Alkali U(VI)-Carbonate Complexes at I = 0.33 M (Converted to Molality), as well as Estimated Electrophoretic Mobilities μ_i Based on a Q Value of 0.63×10^4 Vs/cm^2[a]

species	$\mu/10^{-4}$ cm^2/(Vs)	$\log \beta_{Li}^{0.335m}$	$\log \beta_{Na}^{0.333m}$	$\log \beta_{K}^{0.332m}$
$UO_2^+ + UO_2Cl^+$	3.09			
$UO_2(CO_3)_{(aq)}$	0	9.74 ± 0.25	9.50 ± 0.12	9.89 ± 0.18
$UO_2(CO_3)_2^{2-}$	−3.17	17.70 ± 0.28	17.32 ± 0.22	17.77 ± 0.20
$UO_2(CO_3)_3^{4-}$	−6.35	24.23 ± 0.58	24.57 ± 0.25	24.12 ± 0.25
species	$\mu/10^{-4}$ cm^2/(Vs)	$\log K_{Li}^{0.335m}$	$\log K_{Na}^{0.333m}$	$\log K_{K}^{0.332m}$
$MeUO_2(CO_3)_3^{3-}$	−4.76	−0.16	0.22	0.74
$Me_2UO_2(CO_3)_3^{2-}$	−3.17	1.42	1.34	1.24

[a]Adding the Me-U(VI)-CO_3 complexes to the fit enables the estimation of the mobilities of all complexes with a Q value of 0.63×10^4 Vs/cm^2.

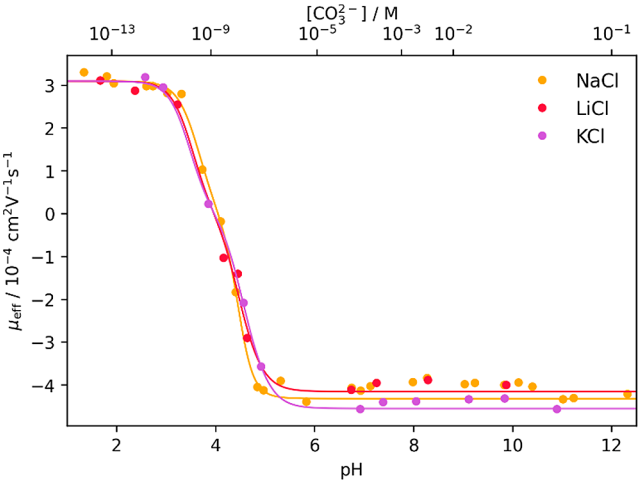

Figure 5. Measured effective electrophoretic mobilities μ_{eff} of ^{238}U(VI) in LiCl, NaCl, and KCl plotted against the pH value and the free carbonate concentration $[CO_3^{2-}]$ at I = 0.33 M with applied fit (solid lines) according to eq 21. R_{Li}^2 = 0.993, R_{Na}^2 = 0.996, and R_K^2 = 0.999.

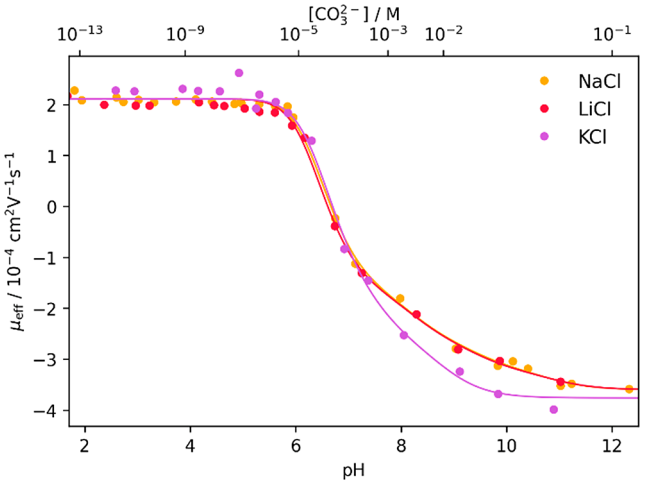

Figure 6. Measured effective electrophoretic mobilities μ_{eff} of ^{237}Np(V) in LiCl, NaCl, and KCl plotted against the pH value and the free carbonate concentration $[CO_3^{2-}]$ at I = 0.33 M with applied fit according to eq S2. R_{Li}^2 = 0.998, R_{Na}^2 = 0.998, and R_K^2 = 0.994.

determined without consideration of the ternary alkali complexes. Although for Na^+ the β_3 value is still about two orders of magnitude higher than the literature value, it is now closer to the literature,[5] indicating an improvement of the model by including the alkali complexes.

Speciation diagrams for U(VI) under the experimental parameters are shown in Figure S7 (Supporting Information) without and with consideration of the alkali complexes determined in this work. Speciation diagrams were calculated manually only utilizing the constants determined in this work (Tables 5 and 8).

By assuming the formation of alkali uranyl carbonate complexes, the limiting mobility of U(VI) can be well modeled, which shows the consistency of the obtained complex formation constants over the different experiments.

3.2.2. Neptunium. In addition to U(VI), also Am(III), Th(IV), and Np(V) were investigated in $LiCl/Li_2CO_3$ and KCl/K_2CO_3 solutions. For Am(III) and Th(IV), no satisfactory mobility curves could be obtained (not shown here). The trend in effective electrophoretic mobility μ_{eff} for Np(V) in LiCl, NaCl, and KCl is shown in Figure 6. Measurements in LiCl reproduced the measurements in NaCl, while the mobilities in KCl deviate significantly at higher carbonate concentrations. In general, the mobilities follow the trend $|\mu_{Li}| \approx |\mu_{Na}| < |\mu_K|$ as observed for U(VI).

In contrast to U(VI), the carbonate complexation of Np(V) does not reach the point where the limiting carbonate complex is almost 100% present in the investigated concentration range of carbonate. This complicates experiments to determine the alkali association, as at least two carbonate complexes are always present in significant proportions. The trend in electrophoretic mobility in LiCl and KCl was fitted analogously to the NaCl experiment by using the mobilities in Table 2. The complex formation constants $\log \beta_i$ for the three Np(V) carbonate complexes at I = 0.33 M (converted to molality) are summarized in Table 9.

The $\log \beta_i$ values for the 1:1 complex in Table 9 coincide with each other regardless of the alkali cation, indicating a negligible influence of the alkali cation. For the 1:2 and 1:3 complexes, the $\log \beta_i$ values for Li^+ and Na^+ also coincide with

Table 9. Complex Formation Constants $\log \beta_i$ for Np(V)-Carbonate Complexes at I = 0.33 M LiCl, NaCl, and KCl (Converted to Molality), Calculated Using the Individual Mobilities of the Species in Table 2, Disregarding the Me-Np(V)-CO_3 Complexes

species	$\log \beta_{Li}^{0.335m}$	$\log \beta_{Na}^{0.333m}$	$\log \beta_{K}^{0.332m}$
$NpO_2(CO_3)^-$	4.31 ± 0.04	4.24 ± 0.04	4.21 ± 0.09
$NpO_2(CO_3)_2^{3-}$	6.77 ± 0.16	6.68 ± 0.14	7.30 ± 0.20
$NpO_2(CO_3)_3^{5-}$	7.65 ± 0.31	7.51 ± 0.23	9.18 ± 0.27
$NpO_2(CO_3)_2OH^{4-}$	−3.85 ± 0.74	−3.88 ± 0.42	-

https://doi.org/10.1021/acs.inorgchem.5c02509
Inorg. Chem. 2025, 64, 20915−20926

Table 10. Complex Formation Constants $\log \beta_i$ for Np(V)-Carbonate Complexes and $\log K_i$ for Alkali Np(V)-Carbonate Complexes at I = 0.33 M as well as Estimated Electrophoretic Mobilities μ_i Based on a Q Value of 0.63 × 10^4 Vs/cm^2, under the Consideration of Me-Np(V)-CO_3 Complexes

species	$\mu/10^{-4}$ cm^2/(Vs)	$\log \beta_{Li}^{0.335m}$	$\log \beta_{Na}^{0.333m}$	$\log \beta_{K}^{0.332m}$
$NpO_2^+ + NpO_2Cl_{(aq)}$	2.11			
$NpO_2(CO_3)^-$	−1.59	4.34 ± 0.05	4.25 ± 0.04	4.25 ± 0.09
$NpO_2(CO_3)_2^{3-}$	−4.76	6.25 ± 0.17	6.13 ± 0.15	6.17 ± 0.52
species	$\mu/10^{-4}$ cm^2/(Vs)	$\log K_{Li}^{0.335m}$	$\log K_{Na}^{0.333m}$	$\log K_{K}^{0.333m}$
$MeNpO_2(CO_3)_2^{2-}$	−3.17	-	-	1.40 ± 0.71
$Me_2NpO_2(CO_3)_2^-$	−1.59	1.03 ± 0.19	1.01 ± 0.17	-

each other but show a significant deviation for K^+. This suggests that the highly negatively charged Np(V) carbonate or hydroxide carbonate complexes also form associated complexes with the alkali cations, analogous to U(VI).

Because of this effect, ternary Me-Np(V)-CO_3 complexes were also included in the fit equation for the Np(V) system (eqs S3 and S4, Supporting Information). To simplify the system, the range of carbonate concentration considered was limited to a maximum of 2 × 10^{-2} M. Thus, the influence of the 1:3 and 1:2:OH complexes can be neglected (see speciation Figure S8, Supporting Information). Analogous to U(VI), $MeNpO_2(CO_3)_2^{2-}$ and $Me_2NpO_2(CO_3)_2^-$ were considered as potential associated complexes. Because the experiment was conducted at a constant $[Me^+]$ of 0.3 M, it was not possible to produce a stable fit considering both complexes at the same time. Both stoichiometries were fitted separately based on the following equilibria

$$K_1: \quad Me^+ + NpO_2(CO_3)_2^{3-} \rightleftharpoons MeNpO_2(CO_3)_2^{2-} \tag{22}$$

$$K_2: \quad 2Me^+ + NpO_2(CO_3)_2^{3-} \rightleftharpoons Me_2NpO_2(CO_3)_2^- \tag{23}$$

Except for μ_0, all electrophoretic mobilities of the Np(V) species were calculated with a Q value of 0.63 × 10^{-4} Vs/cm^2 and were fixed during the fitting procedure. The value for μ_0 was again derived from the plateau at low $[CO_3^{2-}]$ in NaCl. The results for each fit are shown in the SI (Tables S3 and S4, Figures S9 and S10, Supporting Information). The results from the most plausible fits are summarized in Table 10.

For K^+, the addition of the $MeNpO_2(CO_3)_2^{2-}$ complex produces the most plausible log β_i values with both values for the 1:1 and 1:2 complexes agreeing with the literature[2] within the margin of error. For Li^+ and Na^+, the addition of the $MeNpO_2(CO_3)_2^{2-}$ complex (Table S3, Supporting Information) underestimates the β_i value of the 1:2 complex by one to two orders of magnitude compared to literature.[2] The $Me_2NpO_2(CO_3)_2^-$ complex better describes the charge compensation that is observed for Li^+ and Na^+. By adding this complex for Li^+ and Na^+, the log β_i values for the 1:1 and 1:2 Np(V)-CO_3 complexes coincide with each other regardless of the alkali cation and are in range of the literature.[2] The estimated complex formation constants for the $Me_2NpO_2(CO_3)_2^-$ complex with Li^+ and Na^+ are identical. Note that the estimation only considers one associated complex and the preceding alkali complex was neglected. Thus, the log K value of the $Me_2NpO_2(CO_3)_2^-$ complexes could be overestimated.

4. CONCLUSION

With the coupling between CE and ICP-MS, it was possible to determine formation constants for the carbonate complexes of Am(III), Th(IV), Np(V), and U(VI) simultaneously at low concentrations (μM). This enabled the investigation of only mononuclear actinide carbonate complexes. For Am(III) and Np(V), literature values could be reproduced for the most part. The carbonate complexation of U(VI) was found to be stronger than previously reported in literature. It was not possible to measure Th(IV) with enough certainty to determine complex formation constants, but the observed trend in electrophoretic mobility at pH > 5 was as expected based on literature data.

The sensitivity of the CE-ICP-MS to the charge of a complex allows investigations of association reactions, which would go unnoticed using other methods for speciation in liquid phases. For highly negatively charged actinide-carbonate complexes, a significant influence of alkali cations on the electrophoretic mobility was observed. This effect could be attributed to the association of cations to those complexes. The electrophoretic mobility of negatively charged An-CO_3 complexes was found to follow the trend $|\mu_{Li}| \leq |\mu_{Na}| < |\mu_K|$. Furthermore, the reaction of $UO_2(CO_3)_3^{4-}$ with different alkali cations (Li^+−Cs^+) was studied. The complex formation constants of $MeUO_2(CO_3)_3^{3-}$ and $Me_2UO_2(CO_3)_3^{2-}$ for all investigated cations were determined. A similar influence of alkali cations (Li^+−K^+) on the carbonate complexation of Np(V) was observed and complex formation constants of $KNpO_2(CO_3)_2^{2-}$ and $Me_2NpO_2(CO_3)_2^-$ for Li^+ and Na^+ were estimated.

More work is needed to understand the role of cations in the electrolyte, which are no longer seen as innocent bystanders but rather seem to take part in the reaction. Even though CE-ICP-MS proved to be a powerful tool for investigating these cation interactions, more experiments and molecular dynamics calculations are needed to further investigate ternary alkali-actinide-carbonate complexes in solution.

■ ASSOCIATED CONTENT

Supporting Information

The Supporting Information is available free of charge at https://pubs.acs.org/doi/10.1021/acs.inorgchem.5c02509.

Additional CE-ICP-MS data, speciation diagrams, experimental parameters, and electropherograms (PDF)

■ AUTHOR INFORMATION

Corresponding Author

Tobias Reich − *Johannes Gutenberg-Universität Mainz, Department of Chemistry-Nuclear Chemistry, 55099 Mainz, Germany;* orcid.org/0000-0002-5600-3951; Email: treich@uni-mainz.de

https://doi.org/10.1021/acs.inorgchem.5c02509
Inorg. Chem. 2025, 64, 20915−20926

Authors

Janik Lohmann − *Johannes Gutenberg-Universität Mainz, Department of Chemistry-Nuclear Chemistry, 55099 Mainz, Germany;* orcid.org/0009-0002-1610-6339

Stefanie Isabella Demel − *Johannes Gutenberg-Universität Mainz, Department of Chemistry-Nuclear Chemistry, 55099 Mainz, Germany*

Justus Carl Sander − *Johannes Gutenberg-Universität Mainz, Department of Chemistry-Nuclear Chemistry, 55099 Mainz, Germany;* orcid.org/0009-0009-9680-6829

Complete contact information is available at: https://pubs.acs.org/10.1021/acs.inorgchem.5c02509

Author Contributions

J.L.: writing—original draft, writing—review and editing, visualization, methodology, conceptualization, investigation, formal analysis, project administration. S.I.D.: review and editing, investigation. J.C.S.: review and editing, investigation. T.R.: writing—review and editing, conceptualization, methodology, resources, supervision, project administration, funding acquisition

Funding

This project was in part funded by the Federal Ministry for the Environment, Nature Conservation, Nuclear Safety and Consumer Protection (BMUV) under contract no. 02E11860A.

Notes

The authors declare no competing financial interest.

■ ACKNOWLEDGMENTS

The authors would like to thank Dr. Samer Amayri, Dr. Janina Stietz, Dr. Jean Aupiais, and Felix Berg for their contributions during fruitful discussions. The authors would also like to thank the three anonymous reviewers, whose comments helped to improve the manuscript.

■ REFERENCES

(1) Runde, W. Geochemical Interactions of Actinides in the Environment. In *Geochemistry of Soil Radionuclides*; Zhang, P.-C.; Brady, P. V., Eds.; SSSA Special Publications; Soil Science Society of America, 2002; pp 21−44.

(2) Lemire, R. J.; Fuger, J.; Nitsche, H.; Potter, P.; Rand, M. H.; Rydberg, J.; Spahiu, K.; Sullivan, J. C.; Ullman, W. J.; Vitorge, P.; Wanner, H. Chemical Thermodynamics of Neptunium and Plutonium. In *Chemical Thermodynamics*; OECD Publishing, 2001; Vol. *4*.

(3) Guillaumont, R.; Fanghänel, T.; Fuger, J.; Grenthe, I.; Neck, V.; Palmer, D. A.; Rand, M. H. Update on the Chemical Thermodynamics of Uranium, Neptunium, Plutonium, Americium and Technetium. In *Chemical Thermodynamics*; OECD Publishing, 2003; Vol. *5*.

(4) Rand, M.; Fuger, J.; Grenthe, I.; Neck, V.; Rai, D. Chemical Thermodynamics of Thorium. In *Chemical Thermodynamics*; OECD Publishing, 2009; Vol. *11*.

(5) Grenthe, I.; Gaona, X.; Plyasunov, A. V.; Rao, L.; Runde, W. H.; Grambow, B.; Konings, R. J. M.; Smith, A. L.; Moore, E. E. Second Update on the Chemical Thermodynamics of U, Np, Pu, Am and Tc. In *Chemical Thermodynamics*; OECD Publishing, 2020; Vol. *14*.

(6) Pearson, F. J. *Opalinus Clay Experimental Water: A1 Type, Version 980318; Internal Technical Report TM-44−98−07*; Paul Scherrer Institut: Villigen PSI, Switzerland, 1998.

(7) Felmy, A. R.; Rai, D.; Fulton, R. W. The Solubility of $AmOHCO_3(c)$ and the Aqueous Thermodynamics of the System Na^+-Am^{3+}-HCO_3^--CO_3^{2-}-OH^--H_2O. *Radiochim. Acta* **1990**, *50* (4), 193−204.

(8) Nitsche, H.; Standifer, E. M. Americium(III) Carbonate Complexation in Aqueous Perchlorate Solution. *Radiochim. Acta* **1989**, *46* (4), 185−190.

(9) Fanghänel, T.; Weger, HT.; Könnecke, T.; Neck, V.; Paviet-Hartmann, P.; Steinle, E.; Kim, J. I. Thermodynamics of Cm(III) in Concentrated Electrolyte Solutions. Carbonate Complexation at Constant Ionic Strength (1 m NaCl). *Radiochim. Acta* **1998**, *82* (s1), 47−54.

(10) Fanghänel, T.; Könnecke, T.; Weger, H.; Paviet-Hartmann, P.; Neck, V.; Kim, J. I. Thermodynamics of Cm(III) in Concentrated Salt Solutions: Carbonate Complexation in NaCl Solution at 25°C. *J. Solution Chem.* **1999**, *28* (4), 447−462.

(11) Altmaier, M.; Neck, V.; Müller, R.; Fanghänel, T. Solubility of $ThO_2{\cdot}xH_2O(am)$ in Carbonate Solution and the Formation of Ternary Th(IV) Hydroxide-Carbonate Complexes. *Radiochim. Acta* **2005**, *93* (2), 83−92.

(12) Altmaier, M.; Neck, V.; Denecke, M. A.; Yin, R.; Fanghänel, T. Solubility of $ThO_2{\cdot}xH_2O(am)$ and the Formation of Ternary Th(IV) Hydroxide-Carbonate Complexes in $NaHCO_3$-Na_2CO_3 Solutions Containing 0−4 M NaCl. *Radiochim. Acta* **2006**, *94* (9−11), 495−500.

(13) Östhols, E.; Bruno, J.; Grenthe, I. On the Influence of Carbonate on Mineral Dissolution: III. The Solubility of Microcrystalline ThO_2 in CO_2-H_2O Media. *Geochim. Cosmochim. Acta* **1994**, *58* (2), 613−623.

(14) Topin, S.; Aupiais, J.; Moisy, P. Direct Determination of Plutonium(V) and Neptunium(V) Complexation by Carbonate Ligand with CE-ICP-Sector Field MS. *Electrophoresis* **2009**, *30* (10), 1747−1755.

(15) Aupiais, J.; Alexandre, J.-C.; Sicre, R.; Siberchicot, B.; Topin, S.; Moisy, P.; Dacheux, N. The Np^V and Pu^V Carbonate Systems: Thermodynamics and Coordination Chemistry. *Eur. J. Inorg. Chem.* **2020**, *2020* (2), 216−225.

(16) Pashalidis, I.; Czerwinski, K. R.; Fanghänel, T.; Kim, J. I. Solid-Liquid Phase Equilibria of Pu(VI) and U(VI) in Aqueous Carbonate Systems. Determination of Stability Constants. *Radiochim. Acta* **1997**, *76* (1−2), 55−62.

(17) Meinrath, G.; Klenze, R.; Kim, J. I. Direct Spectroscopic Speciation of Uranium(VI) in Carbonate Solutions. *Radiochim. Acta* **1996**, *74* (s1), 81−86.

(18) Kato, Y.; Meinrath, G.; Kimura, T.; Yoshida, Z. A Study of U(VI) Hydrolysis and Carbonate Complexation by Time-Resolved Laser-Induced Fluorescence Spectroscopy (TRLFS). *Radiochim. Acta* **1994**, *64* (2), 107−112.

(19) Willberger, C.; Leichtfuß, D.; Amayri, S.; Reich, T. Determination of the Stability Constants of the Acetate Complexes of the Actinides Am(III), Th(IV), Np(V), and U(VI) Using Capillary Electrophoresis-Inductively Coupled Plasma Mass Spectrometry. *Inorg. Chem.* **2019**, *58* (8), 4851−4858.

(20) Philippini, V.; Vercouter, T.; Aupiais, J.; Topin, S.; Ambard, C.; Chaussé, A.; Vitorge, P. Evidence of Different Stoichiometries for the Limiting Carbonate Complexes Across the Lanthanide(III) Series: a Capillary Electrophoresis-Mass Spectrometry Study. *Electrophoresis* **2008**, *29* (10), 2041−2050.

(21) Grenthe, I.; Mompean, F.; Spahiu, K.; Wanner, H. *Guidelines for the Extrapolation to Zero Ionic Strength*; OECD Publishing, 2013; Vol. *2*.

(22) Good, N. E.; Winget, G. D.; Winter, W.; Connolly, T. N.; Izawa, S.; Singh, R. M. Hydrogen Ion Buffers for Biological Research. *Biochemistry* **1966**, *5* (2), 467−477.

(23) Goldberg, R. N.; Kishore, N.; Lennen, R. M. Thermodynamic Quantities for the Ionization Reactions of Buffers. *J. Phys. Chem. Ref. Data* **2002**, *31* (2), 231−370.

(24) Głab, S.; Hulanicki, A.; Nowicka, U. Coulometric Titration in the Study of Metal Ion-Ligand Equilibria. *Talanta* **1992**, *39* (11), 1555−1559.

(25) Mandal, P.; Kretzschmar, J.; Drobot, B. Not Just a Background: pH Buffers Do Interact with Lanthanide Ions-A Europium(III) Case Study. *J. Biol. Inorg. Chem.* **2022**, *27* (2), 249−260.
(26) Newville, M.; Stensitzki, T.; Allen, D. B.; Ingargiola, A. LMFIT: Non-Linear Least-Square Minimization and Curve-Fitting for Python *Zenodo* 2014.
(27) Novotny, P.; Sohnel, O. Densities of Binary Aqueous Solutions of 306 Inorganic Substances. *J. Chem. Eng. Data* **1988**, *33* (1), 49−55.
(28) Parkhurst, D.; Appelo, C. *Description of Input and Examples for PHREEQC Version 3-A Computer Program for Speciation, Batch-Reaction, One-Dimensional Transport, and Inverse Geochemical Calculations6*; U.S. Geological Survey Techniques and Methods, 2013.
(29) Madé, B.; Bower, W.; Brassinnes, S.; Colàs, E.; Duro, L.; Blanc, P.; Lassin, A.; Harvey, L.; Begg, J. D. Recent Developments in ThermoChimie − A Thermodynamic Database Used in Radioactive Waste Management. *Appl. Geochem.* **2025**, *180*, No. 106273.
(30) Chung, K. H.; Klenze, R.; Park, K. K.; Paviet-Hartmann, P.; Kim, J. I. A Study of the Surface Sorption Process of Cm(III) on Silica by Time-Resolved Laser Fluorescence Spectroscopy (I). *Radiochim. Acta* **1998**, *82* (s1), 215−220.
(31) Bidoglio, G.; Cavalli, P.; Grenthe, I.; Omenetto, N.; Qi, P.; Tanet, G. Studies on Metal Carbonate Equilibria-Part 21 Study of the U(VI)-H_2O-CO_2(g) System by Thermal Lensing Spectrophotometry. *Talanta* **1991**, *38* (4), 433−437.
(32) Edroth, B.; Tommila, E.; Liljenzin, J. O.; Reinhardt, H.; Rydberg, J.; Craig, J. C. Adsorption of Thorium and its TTA-complexes from Aqueous Solutions. *Acta Chem. Scand.* **1969**, *23*, 2636−2640.
(33) Östhols, E. Thorium Sorption on Amorphous Silica. *Geochim. Cosmochim. Acta* **1995**, *59* (7), 1235−1249.
(34) Sun, R.; Dupuis, E.; Aupiais, J.; Reiller, P. E. Study of $Ca_nUO_2(CO_3)_3^{(4-2n)-}$ Complexes using CE-ICP-MS with Polyether-etherketone (PEEK) Capillaries. *Dalton Trans.* **2025**, *54*, 719−727.
(35) Hennig, C.; Ikeda-Ohno, A.; Emmerling, F.; Kraus, W.; Bernhard, G. Comparative Investigation of the Solution Species $U(CO_3)_5^{6-}$ and the Crystal Structure of $Na_6U(CO_3)_5 \cdot 12H_2O$. *Dalton Trans.* **2010**, *39* (15), 3744−3750.
(36) Clark, D. L.; Conradson, S. D.; Ekberg, S. A.; Hess, N. J.; Neu, M. P.; Palmer, P. D.; Runde, W.; Tait, C. D. EXAFS Studies of Pentavalent Neptunium Carbonato Complexes. Structural Elucidation of the Principal Constituents of Neptunium in Groundwater Environments. *J. Am. Chem. Soc.* **1996**, *118* (8), 2089−2090.
(37) Bernhard, G.; Geipel, G.; Reich, T.; Brendler, V.; Amayri, S.; Nitsche, H. Uranyl(VI) Carbonate Complex Formation: Validation of the $Ca_2UO_2(CO_3)_3$(aq.) Species. *Radiochim. Acta* **2001**, *89* (8), 511−518.
(38) Li, X.-B.; Wu, Q.-Y.; Wang, C.-Z.; Lan, J.-H.; Ning, S.-Y.; Wei, Y.-Z. Theoretical Study on Structures of Am(III) Carbonate Complexes. *J. Radioanal. Nucl. Chem.* **2020**, *325* (2), 527−535.
(39) Kelly, S. D.; Kemner, K. M.; Brooks, S. C. X-ray Absorption Spectroscopy Identifies Calcium-Uranyl-Carbonate Complexes at Environmental Concentrations. *Geochim. Cosmochim. Acta* **2007**, *71* (4), 821−834.
(40) Li, B.; Zhou, J.; Priest, C.; Jiang, D.-E. Effect of Salt on the Uranyl Binding with Carbonate and Calcium Ions in Aqueous Solutions. *J. Phys. Chem. B* **2017**, *121* (34), 8171−8178.
(41) Shannon, R. D. Revised Effective Ionic Radii and Systematic Studies of Interatomic Distances in Halides and Chalcogenides. *Acta Cryst. A* **1976**, *32* (5), 751−767.

https://doi.org/10.1021/acs.inorgchem.5c02509
Inorg. Chem. 2025, 64, 20915−20926